Journal of Environmental Chemical Engineering 10 (2022) 108880

Contents lists available at ScienceDirect

Journal of Environmental Chemical Engineering

journal homepage: www.elsevier.com/locate/jece

Experimental evaluation and application of genetic programming to develop predictive correlations for hydrochar higher heating value and yield to optimize the energy content

Nader Marzban [a,b,*,1], Judy A. Libra [a,**,1], Seyyed Hossein Hosseini [c], Marcus G. Fischer [a], Vera Susanne Rotter [b]

[a] Leibniz Institute of Agricultural Engineering and Bio-economy e.V. (ATB), Max-Eyth-Allee 100, 14469 Potsdam, Germany
[b] Department of Environmental Technology, Chair of Circular Economy and Recycling Technology, Technische Universität Berlin, 10623 Berlin, Germany
[c] Department of Chemical Engineering, Ilam University, Ilam 69315−516, Iran

ARTICLE INFO

Editor: Chao He

Keywords:
Hydrothermal carbonization
HHV
Solid yield
Energy yield
Genetic programming
Optimization

ABSTRACT

The hydrothermal carbonization (HTC) process has been found to consistently improve biomass fuel characteristics by raising the higher heating value (HHV) of the hydrochar as process severity is increased. However, this is usually associated with a decrease in the solid yield (SY) of hydrochar, making it difficult to determine the optimal operating conditions to obtain the highest energy yield (EY), which combines the two parameters. In this study, a graph-based genetic programming (GP) method was used for developing correlations to predict HHV, SY, and EY for hydrochars based on published values from 42 biomasses and a broad range of HTC experimental systems and operating conditions, i.e., 5 ≤ holding time (min) ≤ 2208, 120 ≤ temperature (°C) ≤ 300, and 0.0096 ≤ biomass to water ratio ≤ 0.5. In addition, experiments were carried out with 5 pomaces at 4 temperatures and two reactor scales, 1 L and 18.75 L. The correlations were evaluated using this experimental data set in order to estimate prediction errors in similar experimental systems. The use of the correlations to predict HTC conditions to achieve the maximum EY is demonstrated for three common feedstocks, wheat straw, sewage sludge, and a fruit pomace. The prediction was confirmed experimentally with pomace at the optimized HTC conditions; we observed 6.9 % error between the measured and predicted EY %. The results show that the correlations can be used to predict the optimal operating conditions to produce hydrochar with the desired fuel characteristics with a minimum of actual HTC runs.

Glossary.

Symbol	Description	Units
HHV_{HC}	Higher heating value of hydrochar	MJ/kg
HHV_0	Higher heating value of feedstock	MJ/kg
SY	Solid yield	%
EY	Energy yield	%
t	Time	min
T	Temperature	℃
R	Biomass to water ratio	g/g
AE	Absolute error	–
AAE	Average absolute error	–
BE	Biased error	–
ABE	Average biased error	–
GP	Genetic programming	–
HTC	Hydrothermal carbonization	–
C	Carbon	%
H	Hydrogen	%
N	Nitrogen	%
S	Sulfur	%
A	Ash	%
O	Oxygen	%
Daf	dry ash-free	–
Db	dry basis	–
HHV-Elemental	HHV derived from elemental composition	MJ/kg

(continued on next column)

(continued on next page)

* Corresponding author at: Leibniz Institute of Agricultural Engineering and Bio-economy e.V. (ATB), Max-Eyth-Allee 100, 14469 Potsdam, Germany.
** Corresponding author.
E-mail addresses: nmarzban@atb-potsdam.de (N. Marzban), jlibra@atb-potsdam.de (J.A. Libra).
[1] Fax: (+49)331 5699-849

https://doi.org/10.1016/j.jece.2022.108880
Received 1 August 2022; Received in revised form 4 October 2022; Accepted 27 October 2022
Available online 29 October 2022

(*continued*)

Symbol	Description	Units
HHV-Op	HHV derived from operating condition	MJ/kg
Ash0	Ash of feedstock	%

1. Introduction

Sustainable management concepts are required for the numerous wet organic residues produced in industry, agriculture and municipalities, such as food processing residues, livestock manures, and municipal organic wastes. The process of hydrothermal carbonization (HTC) has often been proposed to turn these wet organic residues into stable carbon-rich material, hydrochar, for fuel applications or other uses [1–3]. Hydrothermal reactions such as dehydration, decarboxylation, and decarbonylation in reactor systems using subcritical water can improve the fuel characteristics of the organic residues by reducing the ratio of oxygen to the carbon content, which increases their calorific or heating value [4,5]. Studies with different feedstocks such as lignocellulosic biomass [6], sewage sludge [5,7], animal [8] and food [9] wastes have reported increases in higher heating values of hydrochars (HHV_{HC}) ranging from 3.0% to 37.8 %. Since the process takes place in water, the energy-intensive step of pre-drying the feedstock is eliminated [6]. The product hydrochar has been found to be require less energy to dewater than the initial feedstock [10]. Using HTC to reduce the cost of transportation, handling, and storage of wet organic residues increases their potential for use as fuel for co-combustion in existing power plants [11], and in other combustion processes [4]. The HTC process conditions determine the effect on the heating value, with higher energy inputs, in terms of process temperatures and holding times, producing hydrochars with higher heating values, but with less mass remaining, i.e. with a lower solid yield [11]. Therefore, the assessment of whether the HTC process is economically feasible for converting organic residues into hydrochar for fuel purposes must include an evaluation of the energy yield, which includes the changes in both the HHV_{HC} and solid yield.

Correlations that allow the prediction of the final HHV values and the expected solid yield from HTC processes would be helpful to estimate the potential benefits to be expected for each feedstock. Since HHV increases with process severity and solid yield decreases, locating the optimal process conditions for the highest energy yield is important for economical operation. The availability of prediction tools would reduce the amount of experimental trial and error required to find the optimum. While many correlations exist for predicting the HHV from the elemental composition of a solid [12,13], very few have proposed general correlations for HHV and/or solid yield (SY) as a function of the operating conditions. Two correlations by Li et al. (2015) were developed for HHV and SY using regression techniques based on a statistical analysis of 263 data points from the literature [14]. However, they have limited practicality because they require an extensive list of input data, which is often not available. Further correlations for HHV [15,16], and for SY [15,17–21] have been derived for single feedstocks in statistically designed experiments and not intended as general correlations to be used for other feedstocks and reactor systems. More recently, machine learning models were developed to predict the HHV and SY [22–24]. Vardiambasis et al. (2020) employed the Artificial Neural Network (ANN) technique to predict the HHV_{HC} and carbon content of hydrochars based on the elemental composition of the feedstock, and the HTC process conditions, temperature and time [3]. However, the artificial neural networks method is unable to give an explicit correlation, which can be used for future predictions. Therefore, developing general HHV_{HC} and SY correlations based on very few input variables that can be used for different feedstocks and a wide range of operating conditions would help to reduce the number of time and effort-consuming HTC runs needed to optimize the energy yield.

In this study, we used an intelligent non-linear based method of genetic programming combined with extensive data collected from literature to develop general correlations that can be used to predict the HHV_{HC} and the SY of the hydrochar for chosen HTC process conditions. Firstly, two correlations to predict the HHV_{HC} were derived, one based on the elemental composition of the hydrochar and the other based on the HTC operating conditions. Secondly, a correlation to predict SY from the operating conditions was developed. The accuracy of these correlations was compared with that of previous correlations, and a sensitivity analysis was made for each correlation to identify the effect of the individual variables on the response. In addition, the correlations were evaluated with an additional experimental data set from the hydrothermal carbonization of 5 biomasses produced in this study. In the last section, we demonstrate how the correlations can be used together to predict the energy yield and to find the optimum process conditions for giving the maximum energy yield. This was done theoretically for two common feedstocks: wheat straw and sewage sludge, and was confirmed experimentally for quince pomace.

2. Material and methods

2.1. Analysis of results

The solid yield (SY) describes the percentage of input mass recovered as hydrochar and was calculated as the ratio of carbonized product in weight (M_C) to raw feedstock weight (M_b).

$$SY = \frac{M_C}{M_b} \times 100 \quad [\%] \tag{1}$$

Similarly, the energy yield is the percentage of the initial energy in the feedstock that is recovered in the hydrochar.

2.2. Energy yield (EY)

$$EY = SY \times \frac{HHV_{HC}}{HHV_0} \quad [\%] \tag{2}$$

Where SY is solid yield, HHV_{HC} and HHV_0 are the higher heating values of product and biomass, respectively.

To compare the prediction accuracy between the different correlations, both the coefficient of determination (R^2) as well as the average absolute error (AAE) and absolute bias error (ABE) were used. Since there are many outliers in the data sets, AAE and ABE are used to describe the prediction accuracy of the correlations, while R^2 indicates how much of the variation in the measured data is explained by the correlations. For each data set and correlation, the errors between the predicted value ($Value^{Predicted}$) and the measured value ($Value^{measured}$) are calculated:

$$\mathbf{AAE} = \frac{1}{n} \sum_{i=1}^{n} \left| \frac{Value_i^{Predicted} - Value_i^{measured}}{Value_i^{measured}} \right| \tag{3}$$

and

$$\mathbf{ABE} = \frac{1}{n} \sum_{i=1}^{n} \frac{Value_i^{Predicted} - Value_i^{measured}}{Value_i^{measured}} \tag{4}$$

where the value is HHV_{HC}, SY and EY.

2.3. Data selection

Literature published in the field of hydrothermal carbonization from October 2008 until May 2020 was reviewed and 35 references were selected that reported sufficient data on experimental HTC process conditions, measured higher heating values, elemental composition of biomass and/or hydrochar, and SY. These contained 298 data points

from 42 feedstocks that could be partially used to develop and test the correlation of HHV based on elemental composition and operating condition, and for SY. Table S1 in supplementary material summarizes the number of data, feedstocks and type of feedstocks used in each correlation. Prior to commencing the study, the data points were converted to the appropriate values (either dry ash-free basis (daf) or dry basis (db)), using X=Y× 100/(100-ash), where Y is the percentage of C, H, N, S and O in db and X the percentages of these elements on daf basis. After collecting all the data points, random numbers generated using MS Excel were assigned to each dataset, and ordered from smallest to largest, then the first 70 % of data was selected for training the correlations and the rest (30 %) for testing. All data points are shown in the final figures for the correlations.

The data set (281 data) collected from [6,13,15,16,20,25–45] for derivation of HHV_{HC} based on the elemental composition of the hydrochar (HHV-Elemental), covers a wide range of measured HHV_{HC} (14.37–33.21 MJ/kg) and elemental composition (wt %, db), i.e. $30.49 \leq C\ \% \leq 76.5$, $2.94 \leq H\ \% \leq 9.4$, $0 \leq N\ \% \leq 10.18$, $0 \leq S\ \% \leq 3.66$, $5 \leq O\ \% \leq 48$, $0 \leq Ash\ \% \leq 43.92$. To develop the correlations based on operation conditions, a wide range of data (298 data) was also available in [6,16,21,25,27,28,30,31–42,44,45–53] (see Figure S1 in Supplementary Information), For the correlation HHV-Operating conditions, the ranges were $13.3 \leq HHV_0$ of biomass (MJ/kg) ≤ 27.7, $5 \leq$ holding time t (min) ≤ 2208, $120 \leq$ temperature T (°C) ≤ 300, $0.0096 \leq$ biomass to water ratio $R \leq 0.5$. Most of this data (281 data) was also used for the prediction of SY, where the measured SY values ranged from 33.32 % and 98.23 %, except the holding time (min) was reduced to 0–1440 min [6,15,16,20,25,27,28,30,31,33–37,41,42,44–48,50,51–53]. The predicted EY values were compared to the so-called measured EY values calculated from the measured HHV_0, HHV_{HC} and SY values.

2.4. Genetic programming (GP)

In the present study, a graph-based GP was used to explore new correlations for predicting the HHV_{HC} and SY. GP was patented by Koza [54] as an evolutionary computing, machine learning or artificial intelligence technique based on a tree representation of genes. In contrast to other intelligent methods, such as artificial neural networks, GP provides an explicit relationship between dependent and independent variables, which is the main advantage of this method. The GP was performed using eureqa toolbox [55] and Figure S2 in supplementary material shows the algorithm used by GP to develop the correlations in this study. More details about GP method can be found elsewhere [56–58]. For the sensitivity analysis of the GP models, the sample Pearson's correlation coefficient was used as the relevance coefficient to determine the effects of the input variables on the model outputs. For each input variable, the relevance coefficient varies between (−1) to (+1), indicating a strongly negative to strongly positive relationship.

2.5. Hydrothermal carbonization

To evaluate the correlations developed by GP in this study, we performed 20 HTC experiments of 5 pomaces, namely, quince, apple, pear, beetroot, carrot, collected from a local company in Havelland, Germany. Since the effect of temperature on HHV and yield of hydrochar is higher than the time and biomass to water ratio, only the temperature was altered from 220, 230, 240 and 250 °C. The biomass to water ratio (R) was held at approximately 0.08 and time at 3 h for all runs. The mixture of water and wet pomace was adjusted to 625 g for all the 20 runs and then transferred into a 1 L Parr stirred reactor (reactor series 4520, Moline, IL, USA). The slurry was heated at a rate of 2 °C/min and stirred continuously at 90 rpm. At the end of the reaction time, the heater was turned off, and the reactor was allowed to cool down to around 46 °C. The slurry was filtered using a vacuum filter paper (ROTH Type 113A-110, 5–8 μm). The solid product was dried in an oven at 105 °C for 24 h, placed into a zip-lock bag and stored for further analyses. To evaluate the effect of scale on the prediction error of the correlations, we performed an example run for quince in a 18.75 L Parr stirred reactor (5 gal, model 4557, Moline, Illinois 61265–1770 USA), at 250 °C and 3 h and the same heating rate as in the 1 L reactor. At the end of reaction, the reactor was cooled down over night. The slurry was filtered with the same procedure as 1 L reactor. Both reactors (1 L and 18.75 L) were filled to approximately 63 % of the reactor's total volume. After deriving the correlations, one extra HTC run was made for quince in 1 L reactor at suggested optimum conditions ($T = 172$ °C, $t = 5$ min, $R=0.3$).

2.5.1. Analysis

A Vario El elemental analyzer (Elementar Analysesysteme, Hanau, Germany) was used to measure the elemental carbon, hydrogen, nitrogen, and sulfur (CHNS) by using the sulfonic acid as a reference. The oxygen content was calculated by difference. Dry matter (DM) was determined at 105 °C for 24 h, while ash was determined at 550 °C for 5 h. The higher heating values (HHVs) of solid samples was measured in IKA Calorimeter C 200-System. The analysis was performed at least two times and the mean values, together with solid and energy yield, which were calculated based on Eq. 1, and 2 can be found in Table S2 in supplemental information.

3. Results and discussion

3.1. HHV_{HC} prediction based on elemental analysis of the hydrochar

For fuel-related applications of hydrochar, a greater HHV improves the efficacy of the combustion and reduces the cost of transportation. Decades of research on a variety of organic solids, ranging from coal to biomass, have shown that it is possible to correlate the elemental composition of an organic solid (i.e. C, H, N, S, A, O) with its experimentally measured HHV [12], (see Table S3 in supplementary material). The correlation is often very specific for the type of solid. Predicting the HHV_{HC} using its elemental composition, which is often routinely measured, reduces the cost of further analysis with the bomb calorimetric method. The correlation extracted by genetic programming from 281 data points for hydrochar produced from 38 feedstocks [6,13,15,16,20,25–45], is a fairly simple equation using the carbon (C) and oxygen (O) content of the hydrochar on a wt %, dry basis to predict the HHV:

$$\mathbf{HHV_{HC} = 0.3853 \times C + \frac{44.98}{O}} \quad (5)$$

where C and O are in wt %, db, and HHV_{HC} in MJ/kg.

This correlation was trained for 196 data with an absolute average error (AAE) of 4.76 % and tested for 85 data points with an AAE of 5.8 %. These correspond to $R^2 = 0.90$ and 0.85 respectively. The close agreement between the errors for the derivation and testing groups, and the closely fitted measured data to the predicted data (Fig. 1) shows that the correlation can be used to predict the HHV_{HC} for a wide range of feedstocks. The correlation evaluated by the pomace experimental data set offers a similar AAE of 5.9 %.

More information about the effect of O and C, on measured and predicted HHV can be found in supplementary information (Figure S3).

3.1.1. Limitation of usage and error estimation of HHV-Elemental correlation

The correlation was developed for hydrochars with HHV values ranging from 14.37 to 33.21 MJ/kg and elemental compositions ranging from $30.49 \leq C \leq 76.5$; $5 \leq O\ \% \leq 48$. (wt %, db). The hydrochars were made from a wide range of feedstocks (38). It can be seen in Fig. 1 that the deviation between predicted and measured HHV_{HC} is higher in some groups of feedstock, e.g. algae and sewage sludge. Closer analysis of the feedstock composition and distribution of the error shows that

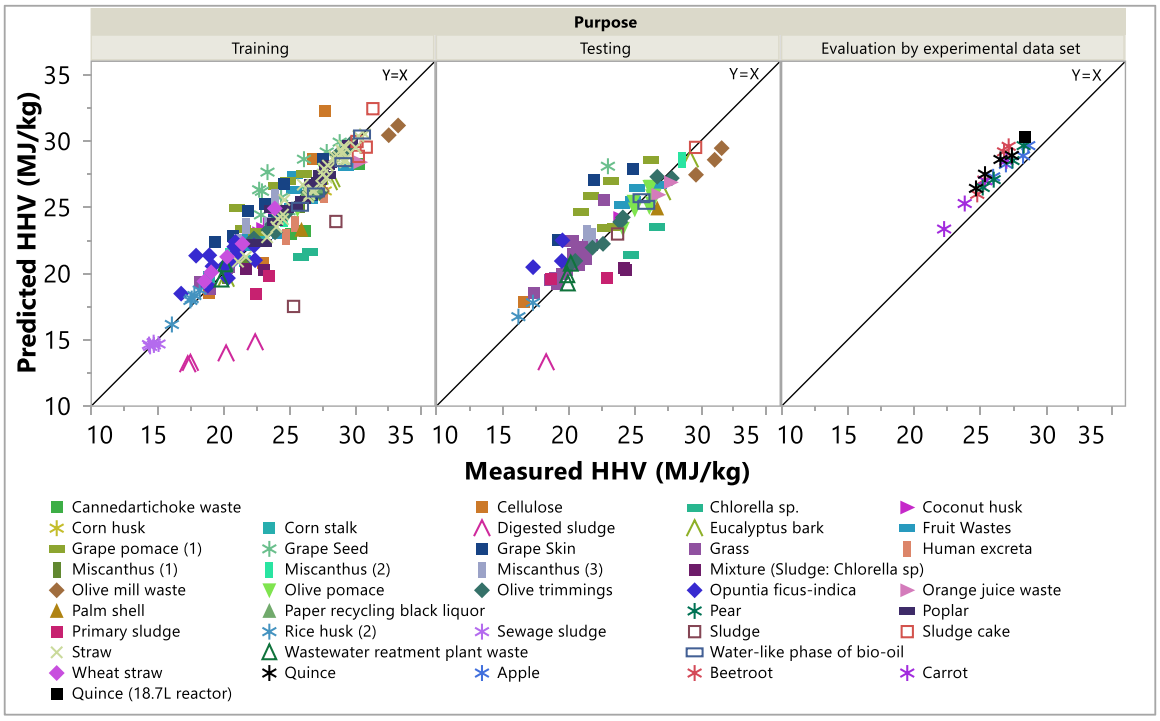

Fig. 1. Comparison between the measured HHV_{HC} from 38 feedstocks and those predicted by the HHV-Elemental correlation, and evaluation of correlation using 21 experimental data.

feedstocks with high ash content contribute more to the error than others (Figures S4 and S5 in the supplementary material). However, not all high ash containing hydrochars have high error. Therefore, the GP correlation (S1) that included A as an input variable did not achieve a lower AAE for all feedstocks than the chosen correlation (see SI and Figure S6 for more discussion). More structural and chemical analyses of the very heterogeneous group of sewage sludge are necessary to identify why some deviate more than others.

3.1.2. *Previous correlations for predicting HHVHC based on elemental analysis*

A literature search returned 23 correlations for predicting HHV from the elemental composition of solids. Most were developed for coals, only a few for biomass, municipal solid waste, or other fuels, and none specifically for hydrochars. The predicted HHV values for the hydrochar data set were calculated with all 23 correlations and the errors (AAE, ABE) were compared. The results for selected correlations collected from [12,59] can be found in Table S3 of the supplementary material. Of the 23 correlations, the widely used correlation by Channiwala and Parikh (2002) [12], which was developed for gaseous, solid and liquid fuels, as well as for biomass and coals, produced the best agreement for the hydrochars (5.4 %). The correlation requires values for H, N, S, ash in addition to C and O. In comparison, our correlation, which was derived with hydrochar values and requires only C and O values, offered the lowest error (5.1 %). The proposed correlation can also predict the HHV for the feedstock (AAE=6.34 %). Interestingly, the more complex correlations (Channiwala, IGT) have slightly smaller errors for the feedstocks.

3.2. *HHV_{HC} prediction based on operating conditions*

Predicting the HHV_{HC} using process condition helps us to design the HTC experiments more efficiently and also gives some overview of the effect of process condition on the HHV_{HC}. Here we are introducing a correlation which can predict the HHV_{HC} taking HTC process conditions such as time, temperature and biomass to water ratio into account. To include the impact of different feedstocks on predicting the HHV of their hydrochars, we considered HHV of feedstock as an input factor for the model. A correlation was trained (AAE=6.4 % and R^2 =0.85) and tested (AAE=8.7 % and R^2 =0.73) using 298 data points and 42 feedstocks as:

$$\mathbf{HHV_{HC}} = \mathbf{HHV_0} + \frac{\mathbf{0.51}}{\mathbf{R} + \mathbf{0.65} \times \mathbf{HHV_0} - \mathbf{10.93}} + \frac{\mathbf{T} + \mathbf{0.0003} \times \mathbf{t} \times \mathbf{T} - \mathbf{143.3}}{\mathbf{HHV_0}} \quad (6)$$

where, t (min) is the holding time at target temperature (°C), R is biomass to water ratio, and HHV_0 is the HHV of feedstock.

Fig. 2 compares the fitness of measured and predicted HHV for different feedstocks. With this correlation, the HHV_{HC} can be calculated without performing the HTC experiments just based on the planned process conditions and the HHV of the feedstock. The pomace experimental data shows close agreement with predicted values, with an AAE of 7.8 %, and the error is less than testing data set. This evaluation shows that the errors found for the training and testing data set are reliable.

3.2.1. *Limitation of usage and error estimation of HHV-OP correlation*

The data set collected for the derivation of this correlation covers a wide range of feedstock and conditions, i.e. 13.3 ≤ HHV_0 of biomass (MJ/kg) ≤ 27.7, 5 ≤ holding time t (min) ≤ 2208, 120 ≤ temperature T (°C) ≤ 300, 0.0096 ≤ biomass to water ratio R ≤ 0.5. In Figure S7, it can be seen that the predicted and measured HHV_{HC} values deviate more for some groups of feedstock, especially animal and industrial wastes, as well as sewage sludge. Similar to the error analysis for the HHV-Elemental correlation, these feedstocks with high ash content contribute more to the error than others (Figure S8). The reactor size in the range studied (15 ml to 4.65 L) and whether the heating system was direct or indirect seem to have little effect on the accuracy of correlation, although the time required for heating up different sized of reactors may vary considerably. However, as can be seen in Figure S8 (in supplementary material), there are no obvious changes in error by using larger reactors, or by the range of operating conditions.

In order to expand the range of reactors studied, the experimental

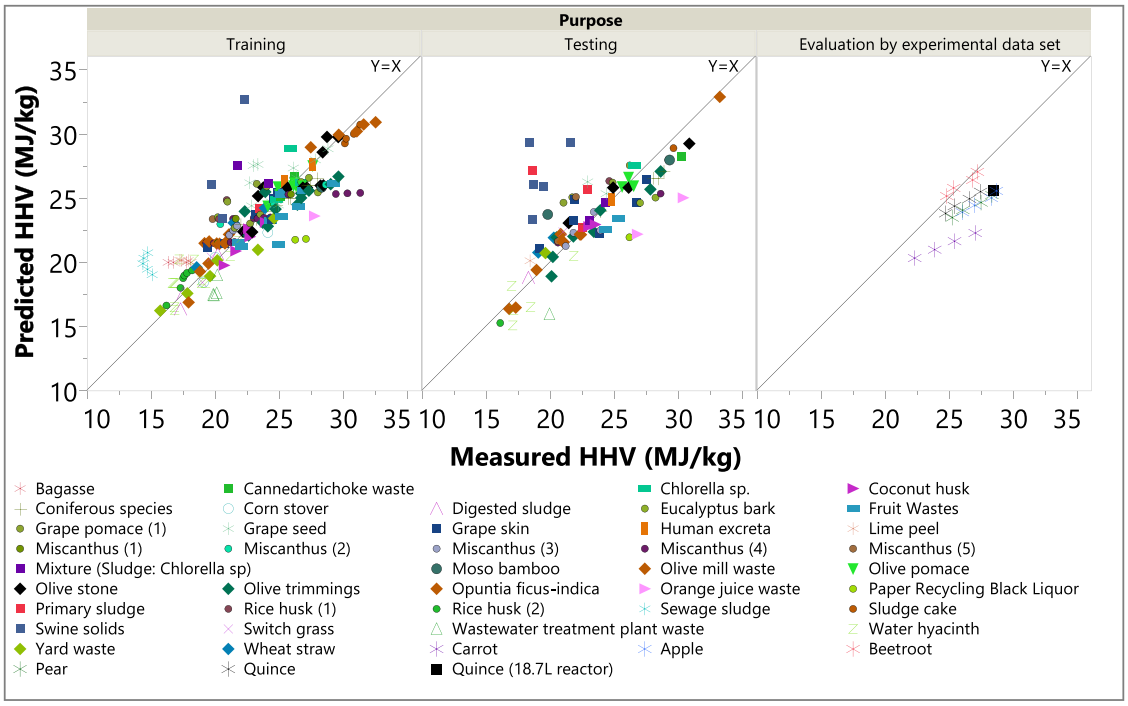

Fig. 2. Comparison between the measured HHV data for hydrochars from 40 feedstocks and those predicted by the HHV-OP correlation based on operating conditions, and evaluation of correlation using 21 experimental data.

results for quince pomace in a 1 L and 18.75 L reactor from this study are compared to predicted values in Table 1. The error difference between the measured and predicted HHV_{HC} produced from the larger scale reactor is very small, 2.8 %. In the future, a broader base of data from large reactors, lab-scale and industrial scale, are needed to improve the correlations. In general, more complete information needs to be published on the reactor systems used, e.g. heat and mass transfer, the type of reactor and feedstock conditions, in order to develop correlations for predicting industrial-scale reactors.

In contrast, for the microwave system, the correlation offers higher error, AAE= 16.2 %. One reason for the high error with microwave-assisted hydrothermal carbonization systems may be that the heat transfer is started from the core of the feedstock particles and expands to the rest of the feedstock and aqueous media. In contrast, with conventional HTC reactor heaters, heat is transferred from the wall of reactor to the aqueous media and then via conduction and convection goes through the feedstock particles. Many factors, such as reaction temperature and material properties such as density, structure and chemical composition, dielectric properties, dipole moments associated with water and other molecules, need to be considered as effective factors in microwave-assisted hydrothermal carbonization [15]. Developing a generalized correlation for microwave-assisted systems that includes the effect of the HHV of feedstock, and three operating parameters, as well as before mentioned factors requires future studies with a wider range of data.

Table 1
Comparison of error between measured and predicted HHV_{HC} produced in 1 L and 18.7 L reactors.

Reactor size (L)	Measured HHV_{HC} (MJ/kg)	Predicted HHV_{HC} (MJ/kg)	ABE %	AAE %
1	27.42	25.44	-7.2	7.2
18.75	28.42	25.5	-10	10

3.2.2. *Previous correlations for predicting HHV_{HC} based on operating conditions*

Our literature search returned three correlations developed to predict HHV_{HC} based on process conditions (Table S4 in supplementary material). The effectiveness and limitations of each correlation were compared with Eq. 6 developed in this study if possible. The first correlation in Table S4 (Li et al.) was developed based on a statistical analysis of 263 data points and requires in addition to t and T, the elemental and proximate analysis of biomass (C, H, A, volatile matter VM, fixed carbon FC), the heating rate HR and time HT and the volume ratio VR [14]. The proximate analysis of biomass and heating rate were not available in most of the selected publications for this study; therefore, we could not predict the HHV_{HC} by this correlation considering the data, which we collected from literature. The correlations reported by Kang et al. (2019) [15], and Volpe et al. (2017) [16], were derived for single feedstocks and were not intended as general correlations to be used for other data, e.g. using coded values for the operating conditions instead of actual values [15]. A test of the correlations with the wide ranging data from 40 feedstocks showed large error. Therefore, we compared the results of our correlation with these two correlations using the small number of data points from each study. Eq. 6 showed higher accuracy compared to the correlation reported by Kang et al. (2019) [15] and close to the predicted results of Volpe et al. (2017) [16]. In conclusion, the HHV-OP correlation needs only values of the HHV of the feedstock and desired process conditions to predict the HHV_{HC} and can be used with ease and high accuracy compared to previous correlations.

3.2.3. *Sensitivity analysis of correlation HHV-OP*

The sensitivity analysis of the HHV-OP correlation clearly shows that the HHV of feedstock has the greatest impact on HHV_{HC} (Figure S9 in supplementary material), while temperature ranks second followed by time and biomass to water ratio. These trends have been seen in other studies [15], although Li et al. found that only time and temperature are statistically significant factors. All input variables have a positive influence on HHV_{HC}.

3.3. Solid yield prediction based on operating conditions

The ability to predict the expected SY of hydrochar for planned operating conditions is a useful tool to design a HTC process efficiently. The following correlation based on the process conditions R, t, and T was derived using 281 data points and 36 feedstocks:

$$\textbf{Solid yield}\% = \mathbf{82.96} + \mathbf{48.95} \times \mathbf{R} - \mathbf{0.01454} \times \mathbf{t} - \mathbf{0.0006} \times \mathbf{T^2} \quad (7)$$

where, t = time (min), T = temperature (°C), R is the biomass to water ratio.

The measured and predicted SY for different feedstocks are compared in Fig. 3. The correlation was trained with 196 data points (AAE=14.6 %; R^2 =0.74) and tested with 85 data points (AAE=13.6 %; R^2 =0.53). The evaluation of correlation using the experimental dataset shows that the higher ash content of feedstocks (e.g., beetroot and carrot) resulted in an overprediction of solid yield. In contrast, the predicted SY for lower ash content feedstocks, like apple and quince, was in close agreement with experimental data.

3.3.1. Limitation of usage and error estimation of the solid yield correlation

The solid yield correlation was developed based on a wide range of process conditions and different feedstocks, where the measured values for SY ranged from 33.32 % and 98.23 %. Most of the data points used to derive the HHV-OP correlation could also be used for this derivation. The data set covers a wide range for the input variables, i.e., $0 \leq$ holding time t (min) ≤ 1440, $120 \leq$ temperature T (°C) ≤ 300, $0.0096 \leq$ biomass to water ratio $R \leq 0.5$, with various reactor sizes and types and feedstocks with ash contents between 0.74 % and 28.6 %. Therefore, the correlation can be used to estimate SY for a wide range of process conditions and feedstocks. However, the accuracy varies between the groups of feedstock (see Figure S10 in the supplementary material). The best prediction with the lowest error is observed for faecal sludge, agro-industrial waste (except corn stalk), fruit and vegetable waste, sewage sludge (Figure S11 in supplementary information). The SY for some individual feedstocks, e.g. corn stover, lime peel and waste eucalyptus bark, were not well-captured by the correlation, being over (+BE %) or under (-BE %) predicted by as much as 40 %. There is again no obvious relationship between the size of reactor and error, similar to what was seen for the HHV-OP correlation.

The correlation offers high error for flash injection (35 %) [49], and continuous reactor systems (47.8 %) [60]. For these systems, the SYs were over predicted. In contrast, the correlation showed high accuracy for batch reactors at two scales with similar heater systems. The comparison between the measured and predicted SY % of 1 L and 18.75 L reactor shows the 4 % higher accuracy of the predicted results of hydrochar produced in 18.75 L (Table 2). More data is required to evaluate whether the correlation developed for laboratory-scale reactors can be applied to predict industrial-scale batch reactors.

For many feedstocks, the correlation follows the trend of the measured SY, but the value is offset. It can be seen in Fig. 3 (and Table S2 in supplementary information) that the higher ash content of carrot and sugar beet biomasses compared to apple, quince and pear, resulted in an over prediction and higher error for SY. A correlation, including a factor to account for ash content may improve the prediction, since the inorganic components of the biomass can be expected to behave differently than the organic components. Unfortunately, the collected data used to train the model did not contain feedstock with gradual changes in ash content. The range between 9 % and 16 % was missing (Figure S12 in supplementary material). To investigate the effect of ash on SY for pomaces, we modeled our experimental data by considering the ash of feedstock and temperature as two variables. The correlation (S2) offered close agreement between experimental and predicted values with an AAE of 1.3 % and R^2 of 0.99 (Figure S13); however, the correlation became more complicated. Increasing the ash of feedstock and T, decreased the SY, whereby the ash content of the biomass showed a higher influence on SY than T. In order to develop a generalized correlation for SY that includes the effect of the three operating parameters, as well as the feedstock ash content on SY future studies with a wider range of data is required.

Table 2
Comparison of error between measured and predicted SY % of two size reactors.

Reactor size (L)	SY % measured	SY % predicted	ABE %	AAE %
1	49.87	46.63	-6	6
18.75	47.00	46.29	-2	2

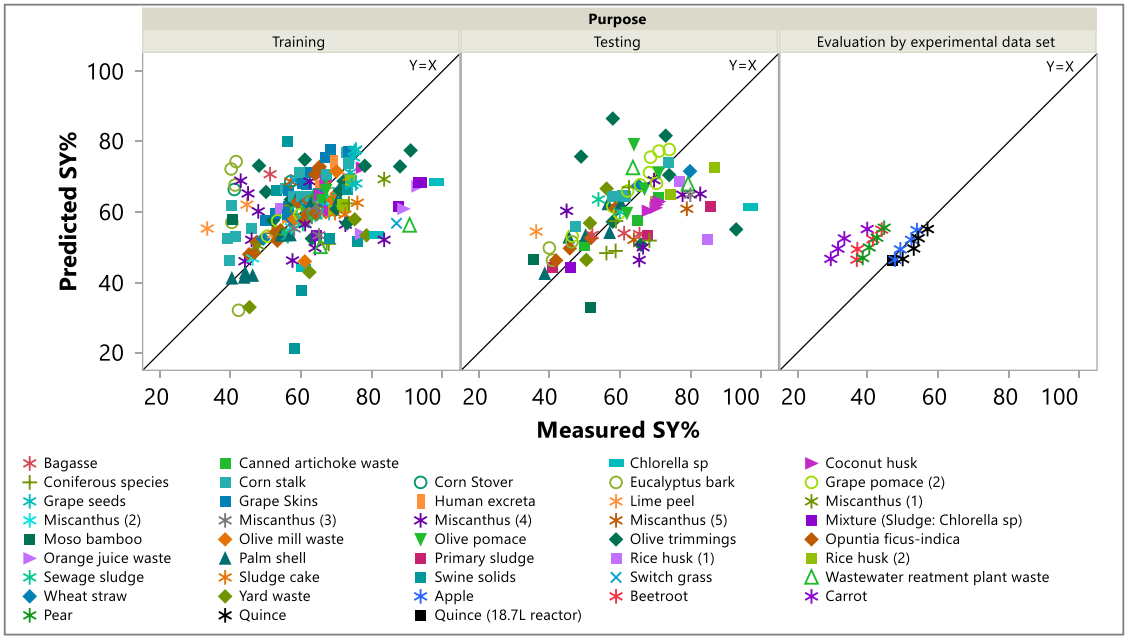

Fig. 3. Comparison between the measured for 36 feedstocks and those predicted by the solid yield correlation based on operating conditions, and evaluation of correlation using 21 experimental data from 5 biomasses.

3.3.2. Previous correlations for predicting solid yield based on operating conditions

Several correlations have been developed to predict the SY of HTC process [14–21,51,61], and we summarized them in Table S5 (see supplementary material). These correlations can be used to predict the solid based on operating conditions. However, only one correlation, Li et al. (2015) [14], is general and developed based on a large number of data points (263) for a wide range of feedstocks. It requires many variables to predict the SY. Since many required input variables are not reported in the literature for the data points we have collected, we could not test their correlation. In contrast, the rest of the correlations (number 2–10) were developed based on a few data points for a single feedstock and were not intended as general correlations. A test of the correlations with the wide-ranging data from our collection showed large error. For six of the correlations (2, 3, 4, 7, 8, 9) the original data was available. Therefore, we compared the results of our correlation with these six correlations using the small number of data points from their respective study. As can be seen in Table 5 S, compared to correlations 4, 7 and 9, our correlation predicted the SY more accurately, while correlations 2, 3, 8 were more accurate compared to our correlation. In conclusion, the SY correlation developed in this study can be used for a wide range of feedstocks and operating conditions while offering relatively low error for most of them.

3.3.3. Sensitivity analysis of correlation for SY based on operating conditions

The sensitivity of the SY prediction to the operating conditions, time, temperature, and biomass-water ratio is shown in Figure S14 (see the supplementary material). Temperature has the greatest impact on SY. Both temperature and time have an inverse relationship with SY, which has been seen in many previous studies [15–21,33,51,62–66]. In contrast, increasing the biomass-water ratio has been usually found to increase the SY [16]. This may be due to greater hydrolysis reactions at lower biomass to water ratios [51]. However, the range of investigated R in most studies is usually narrow and the effect of biomass to water ratio is less evident [17].

3.4. Energy yield prediction based on combining the correlations for HHVHC and SY

Identifying the optimal process conditions to achieve the highest energy yield EY of a hydrochar is important in order to economically operate a HTC system for fuel purposes. The EY is by definition dependent on both the HHV_{HC} and SY at the conditions used in the HTC

Table 3
Algorithms for using correlations to predict the energy yield, and the requirements for energy yield prediction.

Use the HHV-Elemental, HHV-OP and Solid yield correlations	Use the HHV-Elemental, and Solid yield correlations	Use the HHV-OP and Solid yield correlations
Inputs: elemental composition of feedstock, T, t, R	Inputs: elemental composition of feedstock and hydrochar, T, t, R	Inputs: HHV_0, T, t, R
Predict HHV_0 by HHV-Elemental	Predict both HHV_0 and HHV_{HC} by HHV-Elemental	
Predict HHV_{HC} by HHV-Op		Predict HHV_{HC} by HHV-Op
Predict the solid yield	Predict the solid yield	Predict the solid yield
Predict the energy yield	Predict the energy yield	Predict the energy yield
❖ No need to perform HTC runs ❖ We need the elemental composition of feedstock from measurement or literature	❖ Need to perform HTC runs to measure the elemental composition of hydrochar ❖ We need the elemental composition of feedstock and hydrochar	❖ No need to perform HTC runs ❖ We need the HHV of feedstock from measurement or literature

process. However, since HHV_{HC} increases with process severity while SY decreases, determining the optimal EY can be difficult. The correlations developed in the previous sections for HHV_{HC} and SY can be used to search for this optimum before HTC runs are carried out, reducing the amount of experimental trial and error required to find the optimum. Various combinations of the three correlations (HHV-Elemental, HHV-Op and SY) are possible, depending on the data available. In this section, we tested three combinations for their ability to predict the EY of hydrochars made from the various feedstocks and process conditions in the data set. Using the most effective combination, an example is given on how to use the correlations to find the optimum process conditions for three feedstocks to achieve high EY.

3.4.1. Selection of most effective combination of correlations

To predict the energy yield, three combinations of the HHV_{HC} and SY correlations developed in the previous sections were tested against experimental data. Table 3 shows the algorithms for each of the three methods to combine the correlations and their respective input requirements.

Figure S15 (see supplementary material) illustrates the effectiveness of each combination in the prediction of the experimental energy yield. The final energy yield correlations and their errors compared to the 149 measured values from literature and 20 experimental values from this study are summarized in Table 4. The energy yield calculated by combining the HHV-OP and solid yield correlations offered the lowest error compared to the other two combinations (AAE=9.5 %). The advantage of this method is that it can be used to estimate the energy yield of hydrochar without performing any HTC runs. Only a heating value for the feedstock (HHV_0) is required, either from an analysis or literature, and the EY can then be predicted for the desired operating conditions.

3.4.2. Limitation of usage for the energy yield correlations

The correlations can be used to estimate EY for a wide range of process conditions, i.e., $5 \leq$ holding time t (min) ≤ 1440, $120 \leq$ temperature T (°C) ≤ 300, $0.0167 \leq$ biomass to water ratio R ≤ 0.5, and $13.3 \leq HHV_0$ of biomass (MJ/kg) ≤ 27.75 and 18 feedstocks.

3.4.3. Use of the HHV and SY correlations to predict EY

There is general consensus in the literature that the process temperature is the most influential operating parameter on the two important hydrochar characteristics, HHV_{HC} and SY [67]. This was also found in the sensitivity analyses of the correlations developed in this study (Sections 3.2.3 and 3.3.3). In the HHV-OP and solid yield correlations, the two parameters HHV_{HC} and SY are almost linearly dependent on the temperature, as seen in Fig. 4. However, the trends are inversely dependent on temperature. By combining the generalized correlations developed in this paper, it is now possible to find the optimum conditions giving the highest energy yield. Here we illustrate the use of the EY correlation to optimize the HTC process conditions for three common feedstocks, wheat straw, sewage sludge, and a fruit pomace to produce hydrochars with high energy yields. Wheat straw is fairly typical for lignocellulosic feedstocks, the quince pomace is typical for food wastes, while sewage sludge represents feedstocks with high ash and low C-content. The process conditions were selected based on the ranges, which we used to develop both SY and HHV correlations. Table S6 (see supplementary material) shows the range of process conditions studied and the feedstock characteristics for quince pomace of this study, and wheat straw and sewage sludge, taken from [27] and [45] respectively.

To find the optimum conditions, we used the Excel solver to find the maximum energy yield by varying the temperature, time and biomass to water ratio using the EY method based on the HHV-Operating conditions and Solid yield correlations.

The optimum temperature producing the highest EY varied depending on the feedstock (Fig. 4). For both feedstocks, the temperature increased the HHV_{HC} but simultaneously reduced the SY. Results from combining the two correlations to predict EY for wheat straw showed that hydrochar produced at a low temperature, 182 °C, had the highest yield (EY=90.3 %), while for the high ash-containing sewage sludge, 216 °C was optimal (EY=98.6 %). The process conditions for the highest EY were T = 182 °C, t = 5 min, and R= 0.3 for wheat straw and T = 216 °C, t = 509 min, and R= 0.3 for sewage sludge. Theoretically changing the process time had little effect on the optimum yield and temperature. For example, narrowing the range for *t* to 30–300 min, only slightly changed the optimal points for wheat straw (EY=90.2 % for T = 182 °C, t = 30 min) and sewage sludge (EY=98.4 % for T = 220 °C, t = 300 min). The highest EY was calculated for quince as 87.8 % at the optimum condition of T = 172 °C, t = 5 min and R= 0.3. This optimum was experimentally verified with a HTC run at these conditions. Comparison of the predicted to the actual measured EY at optimum condition shows very good agreement, with an error of 6.9 %.

4. Conclusions

In the present study, the intelligent approach of genetic programming (GP) was used as an effective, robust, and smart technique for developing explicit correlations to predict the HHV_{HC} and SY of hydrochar in the HTC process. Two correlations for HHV_{HC} were derived by the GP method using: 1) the elemental composition of the hydrochar (only C, O required), and 2) the HHV of the feedstock and HTC operating conditions. In addition, a correlation for SY based on operating conditions was obtained which can be used together with the HHV_{HC} correlations to predict the energy yield for different biomasses at HTC operating conditions. The correlations were evaluated by additional experimental data sets produced in this study for 5 pomaces, and showed close agreement with the predicted values. Three combinations of the proposed HHV_{HC} and SY correlations reliably predicted the energy yield at different process conditions and an algorithm for the use of the

Table 4
Three possible combinations of the correlations developed in this study to predict the energy yield, and their corresponding errors compared to the 149 measured values from literature and 20 experimental values from this study.

Combination	Energy yield correlations	Errors
Use the HHV-Elemental, and Solid yield correlations	$EY\% = (82.96 + 48.95 \times R - 0.01454 \times t - 0.0006 \times T^2) \times \dfrac{0.3853 \times C \text{ of char} + \dfrac{44.98}{O \text{ of char}}}{0.3853 \times C \text{ of feed} + \dfrac{44.98}{O \text{ of } feed}}$	AAE [%]= 12.0 ABE [%]= 2.8
Use the HHV-OP and Solid yield correlations	$EY\% = (82.96 + 48.95 \times R - 0.01454 \times t - 0.0006 \times T^2) \times \dfrac{HHV_0 + \dfrac{0.51}{R + 0.65 \times HHV_0 - 10.93} + \dfrac{T + 0.0003 \times t \times T - 143.3}{HHV_0}}{HHV_0}$	AAE [%]= 10.6 ABE [%]= 3
Use the HHV-Elemental, HHV-OP and Solid yield correlations	$EY\% = (82.96 + 48.95 \times R - 0.01454 \times t - 0.0006 \times T^2) \times \dfrac{HHV_0 + \dfrac{0.51}{R + 0.65 \times HHV_0 - 10.93} + \dfrac{T + 0.0003 \times t \times T - 143.3}{HHV_0}}{0.3853 \times C \text{ of } feed + \dfrac{44.98}{O \text{ of } feed}}$	AAE [%]= 13.7 ABE [%]= 1.7

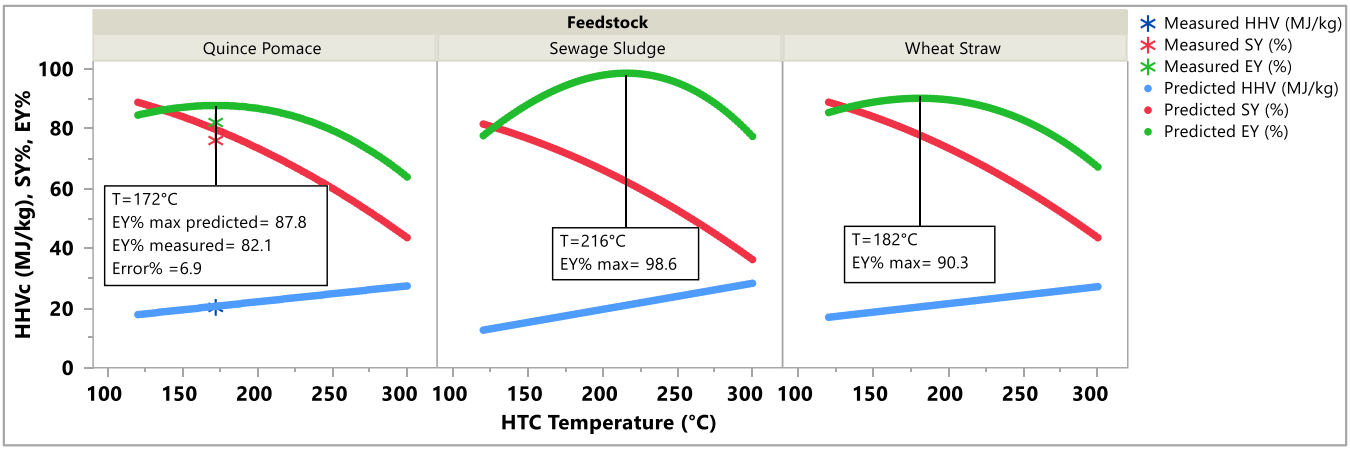

Fig. 4. Evaluation of the optimum HTC conditions to achieve the highest energy yield for three example feedstocks (quince pomace, sewage sludge, and wheat straw) using the EY method based on the HHV-OP and Solid yield correlations.

presented correlations was developed.

The ease of use of the EY correlation to find the maximum EY based on the HHV_0 of the biomass and HTC operating conditions was demonstrated theoretically for two common feedstocks: wheat straw and sewage sludge, and was confirmed experimentally for quince pomace. The advantage of this algorithm is that it can be used to predict the characteristics of hydrochar, such as HHV_{HC}, solid and energy yields, based on feedstock data alone without performing any HTC runs. Since HHV_{HC} increases with process severity and SY decreases, the optimal HTC process conditions for the highest EY was determined by solving both equations simultaneously. Only the feedstock HHV_0 is required, which can usually be found in the literature or easily analyzed. The EY can then be predicted for the desired operating conditions or the operating conditions can be optimized to achieve the highest EY. This can then be checked experimentally at well-selected conditions. Use of this method should help reduce the experimental work required to assess the economic feasibility of using HTC to convert organic residues into hydrochar for fuel applications.

CRediT authorship contribution statement

Nader Marzban: Data collection, Investigation, Modeling, Software, Design of experiments, Formal Analysis, Data curation, Writing – original draft Preparation, Visualization, Conceptualization. **Judy A. Libra:** Supervision, Conceptualization, Methodology, Writing – review & editing, Writing – original draft, Visualization, Project administration, Funding acquisition. **Seyyed Hossein Hosseini:** Methodology, Modeling, Writing – review & editing, Visualization. **Marcus G. Fischer:** Design of experiments, Investigation, Visualization. **Vera Susanne Rotter:** Supervision, Writing – review & editing, Visualization, Conceptualization.

Declaration of Competing Interest

The authors declare that they have no known competing financial interests or personal relationships that could have appeared to influence the work reported in this paper.

Data Availability

Data will be made available on request.

Acknowledgments

We thank the German Academic Exchange Service (DAAD) for providing financial support under the PhD scholarship program (NaWaM).

Appendix A. Supporting information

Supplementary data associated with this article can be found in the online version at doi:10.1016/j.jece.2022.108880.

References

[1] S. Román, J. Libra, N. Berge, E. Sabio, K. Ro, L. Li, B. Ledesma, A. Álvarez, S. Bae, Hydrothermal carbonization: modeling, final properties design and applications: a review, Energies 11 (2018) 216, https://doi.org/10.3390/en11010216.
[2] R. Wang, S. Liu, Q. Xue, K. Lin, Q. Yin, Z. Zhao, Analysis and prediction of characteristics for solid product obtained by hydrothermal carbonization of biomass components, Renew. Energy 183 (2022) 575–585, https://doi.org/10.1016/j.renene.2021.11.001.
[3] I.O. Vardiambasis, T.N. Kapetanakis, C.D. Nikolopoulos, T.K. Trang, T. Tsubota, R. Keyikoglu, A. Khataee, D. Kalderis, Hydrochars as emerging biofuels: recent advances and application of artificial neural networks for the prediction of heating values, Energies 13 (2020) 4572, https://doi.org/10.3390/en13174572.
[4] J.A. Libra, K.S. Ro, C. Kammann, A. Funke, N.D. Berge, Y. Neubauer, M.-M. Titirici, C. Fühner, O. Bens, J. Kern, K.-H. Emmerich, Hydrothermal carbonization of biomass residuals: a comparative review of the chemistry, processes and applications of wet and dry pyrolysis, Biofuels 2 (2011) 71–106, https://doi.org/10.4155/bfs.10.81.
[5] X. Xue, D. Chen, X. Song, X. Dai, Hydrothermal and pyrolysis treatment for sewage sludge: choice from product and from energy benefit1, Energy Procedia 66 (2015) 301–304, https://doi.org/10.1016/j.egypro.2015.02.064.
[6] H.S. Kambo, A. Dutta, Strength, storage, and combustion characteristics of densified lignocellulosic biomass produced via torrefaction and hydrothermal carbonization, Appl. Energy 135 (2014) 182–191, https://doi.org/10.1016/j.apenergy.2014.08.094.
[7] Z. Wang, Y. Zhai, T. Wang, C. Peng, S. Li, B. Wang, X. Liu, C. Li, Effect of temperature on the sulfur fate during hydrothermal carbonization of sewage sludge, Environ. Pollut. 260 (2020), 114067, https://doi.org/10.1016/j.envpol.2020.114067.
[8] K.S. Ro, J.A. Libra, S. Bae, N.D. Berge, J.R.V. Flora, R. Pecenka, Combustion behavior of animal-manure-based hydrochar and pyrochar, ACS Sustain. Chem. Eng. 7 (2019) 470–478, https://doi.org/10.1021/acssuschemeng.8b03926.
[9] H. Su, X. Zhou, R. Zheng, Z. Zhou, Y. Zhang, G. Zhu, C. Yu, D. Hantoko, M. Yan, Hydrothermal carbonization of food waste after oil extraction pre-treatment: Study on hydrochar fuel characteristics, combustion behavior, and removal behavior of sodium and potassium, Sci. Total Environ. 754 (2021), 142192, https://doi.org/10.1016/j.scitotenv.2020.142192.
[10] M. Escala, T. Zumbühl, Ch Koller, R. Junge, R. Krebs, Hydrothermal carbonization as an energy-efficient alternative to established drying technologies for sewage sludge: a feasibility study on a laboratory scale, Energy Fuels 27 (2013) 454–460, https://doi.org/10.1021/ef3015266.
[11] A.T. Mursito, T. Hirajima, K. Sasaki, Upgrading and dewatering of raw tropical peat by hydrothermal treatment, Fuel 89 (2010) 635–641, https://doi.org/10.1016/j.fuel.2009.07.004.
[12] S.A. Channiwala, P.P. Parikh, A unified correlation for estimating HHV of solid, liquid and gaseous fuels, Fuel 81 (2002) 1051–1063, https://doi.org/10.1016/S0016-2361(01)00131-4.
[13] S. Kieseler, Y. Neubauer, N. Zobel, Ultimate and proximate correlations for estimating the higher heating value of hydrothermal solids, Energy Fuels 27 (2013) 908–918, https://doi.org/10.1021/ef301752d.

[14] L. Li, J.R.V. Flora, J.M. Caicedo, N.D. Berge, Investigating the role of feedstock properties and process conditions on products formed during the hydrothermal carbonization of organics using regression techniques, Bioresour. Technol. 187 (2015) 263–274, https://doi.org/10.1016/j.biortech.2015.03.054.
[15] K. Kang, S. Nanda, G. Sun, L. Qiu, Y. Gu, T. Zhang, M. Zhu, R. Sun, Microwave-assisted hydrothermal carbonization of corn stalk for solid biofuel production: Optimization of process parameters and characterization of hydrochar, Energy 186 (2019), 115795, https://doi.org/10.1016/j.energy.2019.07.125.
[16] M. Volpe, J.L. Goldfarb, L. Fiori, Hydrothermal carbonization of Opuntia ficus-indica cladodes: Role of process parameters on hydrochar properties, Bioresour. Technol. 247 (2018) 310–318, https://doi.org/10.1016/j.biortech.2017.09.072.
[17] E. Sabio, A. Álvarez-Murillo, S. Román, B. Ledesma, Conversion of tomato-peel waste into solid fuel by hydrothermal carbonization: Influence of the processing variables, Waste Manag. 47 (2016) 122–132, https://doi.org/10.1016/j.wasman.2015.04.016.
[18] S. Kannan, Y. Gariepy, G.S.V. Raghavan, Optimization and characterization of hydrochar produced from microwave hydrothermal carbonization of fish waste, Waste Manag. 65 (2017) 159–168, https://doi.org/10.1016/j.wasman.2017.04.016.
[19] S. Kannan, Y. Gariepy, G.S.V. Raghavan, Optimization and characterization of hydrochar derived from shrimp waste, Energy Fuels 31 (2017) 4068–4077, https://doi.org/10.1021/acs.energyfuels.7b00093.
[20] S. Nizamuddin, N.M. Mubarak, M. Tiripathi, N.S. Jayakumar, J.N. Sahu, P. Ganesan, Chemical, dielectric and structural characterization of optimized hydrochar produced from hydrothermal carbonization of palm shell, Fuel 163 (2016) 88–97, https://doi.org/10.1016/j.fuel.2015.08.057.
[21] A. Álvarez-Murillo, S. Román, B. Ledesma, E. Sabio, Study of variables in energy densification of olive stone by hydrothermal carbonization, J. Anal. Appl. Pyrolysis 113 (2015) 307–314, https://doi.org/10.1016/j.jaap.2015.01.031.
[22] F. Cheng, M.D. Porter, L.M. Colosi, Is hydrothermal treatment coupled with carbon capture and storage an energy-producing negative emissions technology, Energy Convers. Manag. 203 (2020), 112252, https://doi.org/10.1016/j.enconman.2019.112252.
[23] J. Li, X. Zhu, Y. Li, Y.W. Tong, Y.S. Ok, X. Wang, Multi-task prediction and optimization of hydrochar properties from high-moisture municipal solid waste: Application of machine learning on waste-to-resource, J. Clean. Prod. 278 (2021), 123928, https://doi.org/10.1016/j.jclepro.2020.123928.
[24] L. Li, J.R.V. Flora, N.D. Berge, Predictions of energy recovery from hydrochar generated from the hydrothermal carbonization of organic wastes, Renew. Energy 145 (2020) 1883–1889, https://doi.org/10.1016/j.renene.2019.07.103.
[25] K. Nakason, B. Panyapinyopol, V. Kanokkantapong, N. Viriya-empikul, W. Kraithong, P. Pavasant, Hydrothermal carbonization of unwanted biomass materials: Effect of process temperature and retention time on hydrochar and liquid fraction, J. Energy Inst. 91 (2018) 786–796, https://doi.org/10.1016/j.joei.2017.05.002.
[26] J. Minaret, A. Dutta, Comparison of liquid and vapor hydrothermal carbonization of corn husk for the use as a solid fuel, Bioresour. Technol. 200 (2016) 804–811, https://doi.org/10.1016/j.biortech.2015.11.010.
[27] Q. Ma, L. Han, G. Huang, Effect of water-washing of wheat straw and hydrothermal temperature on its hydrochar evolution and combustion properties, Bioresour. Technol. 269 (2018) 96–103, https://doi.org/10.1016/j.biortech.2018.08.082.
[28] J. Lee, D. Sohn, K. Lee, K.Y. Park, Solid fuel production through hydrothermal carbonization of sewage sludge and microalgae Chlorella sp. from wastewater treatment plant, Chemosphere 230 (2019) 157–163, https://doi.org/10.1016/j.chemosphere.2019.05.066.
[29] D. Kim, K. Yoshikawa, K. Park, Characteristics of biochar obtained by hydrothermal carbonization of cellulose for renewable energy, Energies 8 (2015) 14040–14048, https://doi.org/10.3390/en81212412.
[30] A. Saba, P. Saha, M.T. Reza, Co-Hydrothermal Carbonization of coal-biomass blend: Influence of temperature on solid fuel properties, Fuel Process. Technol. 167 (2017) 711–720, https://doi.org/10.1016/j.fuproc.2017.08.016.
[31] M. Wilk, A. Magdziarz, Hydrothermal carbonization, torrefaction and slow pyrolysis of Miscanthus giganteus, Energy 140, Part 1 (2017) 1292–1304, https://doi.org/10.1016/j.energy.2017.03.031.
[32] B. Zhang, M. Heidari, B. Regmi, S. Salaudeen, P. Arku, M. Thimmannagari, A. Dutta, Hydrothermal carbonization of fruit wastes: a promising technique for generating hydrochar, Energies 11 (2018) 2022, https://doi.org/10.3390/en11082022.
[33] V. Benavente, E. Calabuig, A. Fullana, Upgrading of moist agro-industrial wastes by hydrothermal carbonization, J. Anal. Appl. Pyrolysis 113 (2015) 89–98, https://doi.org/10.1016/j.jaap.2014.11.004.
[34] D. Basso, E. Weiss-Hortala, F. Patuzzi, M. Baratieri, L. Fiori, In deep analysis on the behavior of grape marc constituents during hydrothermal carbonization, Energies 11 (2018) 1379, https://doi.org/10.3390/en11061379.
[35] A. Missaoui, S. Bostyn, V. Belandria, B. Cagnon, B. Sarh, I. Gökalp, Hydrothermal carbonization of dried olive pomace: energy potential and process performances, J. Anal. Appl. Pyrolysis 128 (2017) 281–290, https://doi.org/10.1016/j.jaap.2017.09.022.
[36] M. Lucian, M. Volpe, L. Fiori, Hydrothermal carbonization kinetics of lignocellulosic agro-wastes: experimental data and modeling, Energies 12 (2019) 516, https://doi.org/10.3390/en12030516.
[37] P. Gao, Y. Zhou, F. Meng, Y. Zhang, Z. Liu, W. Zhang, G. Xue, Preparation and characterization of hydrochar from waste eucalyptus bark by hydrothermal carbonization, Energy 97 (2016) 238–245, https://doi.org/10.1016/j.energy.2015.12.123.
[38] Z. Al-Kaabi, R. Pradhan, N. Thevathasan, A. Gordon, Y.W. Chiang, A. Dutta, Bio-carbon production by oxidation and hydrothermal carbonization of paper recycling black liquor, J. Clean. Prod. 213 (2019) 332–341, https://doi.org/10.1016/j.jclepro.2018.12.175.
[39] Y. Fu, J. Ye, J. Chang, H. Lou, X. Zheng, Solid fuel production by hydrothermal carbonization of water-like phase of bio-oil, Fuel 180 (2016) 591–596, https://doi.org/10.1016/j.fuel.2016.04.089.
[40] D. Kim, K. Lee, K.Y. Park, Hydrothermal carbonization of anaerobically digested sludge for solid fuel production and energy recovery, Fuel 130 (2014) 120–125, https://doi.org/10.1016/j.fuel.2014.04.030.
[41] R. Yahav Spitzer, V. Mau, A. Gross, Using hydrothermal carbonization for sustainable treatment and reuse of human excreta, J. Clean. Prod. 205 (2018) 955–963, https://doi.org/10.1016/j.jclepro.2018.09.126.
[42] C. He, A. Giannis, J.-Y. Wang, Conversion of sewage sludge to clean solid fuel using hydrothermal carbonization: hydrochar fuel characteristics and combustion behavior, Appl. Energy 111 (2013) 257–266, https://doi.org/10.1016/j.apenergy.2013.04.084.
[43] T. Koottatep, K. Fakkaew, N. Tajai, S.V. Pradeep, C. Polprasert, Sludge stabilization and energy recovery by hydrothermal carbonization process, Renew. Energy 99 (2016) 978–985, https://doi.org/10.1016/j.renene.2016.07.068.
[44] S.-Y. Oh, Y.-M. Yoon, Energy recovery efficiency of poultry slaughterhouse sludge cake by hydrothermal carbonization, Energies 10 (2017) 1876, https://doi.org/10.3390/en10111876.
[45] D. Bhatt, A. Shrestha, R. Dahal, B. Acharya, P. Basu, R. MacEwen, Hydrothermal carbonization of biosolids from waste water treatment plant, Energies 11 (2018) 2286, https://doi.org/10.3390/en11092286.
[46] S.A. Shafie, K.A. Al-attab, Z.A. Zainal, Effect of hydrothermal and vapothermal carbonization of wet biomass waste on bound moisture removal and combustion characteristics, Appl. Therm. Eng. 139 (2018) 187–195, https://doi.org/10.1016/j.applthermaleng.2018.02.073.
[47] M.T. Reza, J.G. Lynam, M.H. Uddin, C.J. Coronella, Hydrothermal carbonization: fate of inorganics, Biomass-.-. Bioenergy 49 (2013) 86–94, https://doi.org/10.1016/j.biombioe.2012.12.004.
[48] K.S. Ro, J.R.V. Flora, S. Bae, J.A. Libra, N.D. Berge, A. Álvarez-Murillo, L. Li, Properties of animal-manure-based hydrochars and predictions using published models, ACS Sustain. Chem. Eng. 5 (2017) 7317–7324, https://doi.org/10.1021/acssuschemeng.7b01569.
[49] S. Román, B. Ledesma, A. Álvarez, C. Coronella, S.V. Qaramaleki, Suitability of hydrothermal carbonization to convert water hyacinth to added-value products, Renew. Energy 146 (2020) 1649–1658, https://doi.org/10.1016/j.renene.2019.07.157.
[50] H.S. Kambo, A. Dutta, Comparative evaluation of torrefaction and hydrothermal carbonization of lignocellulosic biomass for the production of solid biofuel, Energy Convers. Manag. 105 (2015) 746–755, https://doi.org/10.1016/j.enconman.2015.08.031.
[51] E. Sermyagina, J. Saari, J. Kaikko, E. Vakkilainen, Hydrothermal carbonization of coniferous biomass: effect of process parameters on mass and energy yields, J. Anal. Appl. Pyrolysis 113 (2015) 551–556, https://doi.org/10.1016/j.jaap.2015.03.012.
[52] W. Yan, S. Perez, K. Sheng, Upgrading fuel quality of moso bamboo via low temperature thermochemical treatments: dry torrefaction and hydrothermal carbonization, Fuel 196 (2017) 473–480, https://doi.org/10.1016/j.fuel.2017.02.015.
[53] H.B. Sharma, S. Panigrahi, B.K. Dubey, Hydrothermal carbonization of yard waste for solid bio-fuel production: study on combustion kinetic, energy properties, grindability and flowability of hydrochar, Waste Manag. 91 (2019) 108–119, https://doi.org/10.1016/j.wasman.2019.04.056.
[54] J.R. Koza, Genetic programming: on the programming of computers by means of natural selection, MIT press, 1992.
[55] M. Schmidt, H. Lipson, Distilling Free-form Natural Laws From Experimental Data, Science 324 (2009) 81–85, https://doi.org/10.1126/science.1165893.
[56] S.H. Hosseini, M. Karami, H. Altzibar, M. Olazar, Prediction of pressure drop and minimum spouting velocity in draft tube conical spouted beds using genetic programming approach, Can. J. Chem. Eng. 98 (2020) 583–589, https://doi.org/10.1002/cjce.23590.
[57] N. Marzban, A. Moheb, S. Filonenko, S.H. Hosseini, M.J. Nouri, J.A. Libra, G. Farru, Intelligent modeling and experimental study on methylene blue adsorption by sodium alginate-kaolin beads, Int. J. Biol. Macromol. 186 (2021) 79–91, https://doi.org/10.1016/j.ijbiomac.2021.07.006.
[58] S.H. Hosseini, M.A. Moradkhani, M. Valizadeh, A. Zendehboudi, M. Olazar, A general heat transfer correlation for flow condensation in single port mini and macro channels using genetic programming, S0140700720302760, Int. J. Refrig. (2020), https://doi.org/10.1016/j.ijrefrig.2020.06.021.
[59] C. Sheng, J.L.T. Azevedo, Estimating the higher heating value of biomass fuels from basic analysis data, Biomass-.-. Bioenergy 28 (2005) 499–507, https://doi.org/10.1016/j.biombioe.2004.11.008.
[60] C. Liu, X. Huang, L. Kong, Efficient low temperature hydrothermal carbonization of Chinese reed for biochar with high energy density, Energies 10 (2017) 2094, https://doi.org/10.3390/en10122094.
[61] C. Zhang, C. Zheng, X. Ma, Y. Zhou, J. Wu, Co-hydrothermal carbonization of sewage sludge and banana stalk: fuel properties of hydrochar and environmental risks of heavy metals, J. Environ. Chem. Eng. 9 (2021), 106051, https://doi.org/10.1016/j.jece.2021.106051.
[62] M. Mäkelä, A. Fullana, K. Yoshikawa, Ash behavior during hydrothermal treatment for solid fuel applications. Part 1: overview of different feedstock, Energy Convers. Manag. 121 (2016) 402–408, https://doi.org/10.1016/j.enconman.2016.05.016.

[63] S. Román, J.M.V. Nabais, C. Laginhas, B. Ledesma, J.F. González, Hydrothermal carbonization as an effective way of densifying the energy content of biomass, Fuel Process. Technol. 103 (2012) 78–83, https://doi.org/10.1016/j.fuproc.2011.11.009.

[64] D. Basso, E. Weiss-Hortala, F. Patuzzi, D. Castello, M. Baratieri, L. Fiori, Hydrothermal carbonization of off-specification compost: a byproduct of the organic municipal solid waste treatment, Bioresour. Technol. 182 (2015) 217–224, https://doi.org/10.1016/j.biortech.2015.01.118.

[65] D. Knežević, W. van Swaaij, S. Kersten, Hydrothermal conversion of biomass. II. conversion of wood, pyrolysis oil, and glucose in hot compressed water, Ind. Eng. Chem. Res. 49 (2010) 104–112, https://doi.org/10.1021/ie900964u.

[66] G. Saverettiar, D. Li, A. Gross, G. Ho, Hydrothermal carbonization of cattle paunch waste: process conditions and product characteristics, J. Environ. Chem. Eng. 8 (2020), 104487, https://doi.org/10.1016/j.jece.2020.104487.

[67] A. Funke, F. Ziegler, Hydrothermal carbonization of biomass: a summary and discussion of chemical mechanisms for process engineering, Biofuels, Bioprod. Bioref. 4 (2010) 160–177, https://doi.org/10.1002/bbb.198.